ISBN: 978-3-95450-261-5 ISSN: 2673-7000 doi: 10.18429/JACoW-NAPAC2025-MOP029

DEVELOPMENT AND APPLICATIONS OF DIFFERENTIABLE COHERENT OPTICAL TRANSITION RADIATION SIMULATIONS

R. Roussel*, SLAC National Accelerator Laboratory, Menlo Park, CA, USA
R. Aguilar, M. LaBerge, F. L. Wu, A. Irman, J. Kelling, U. Schramm,
Helmholtz-Zentrum Dresden-Rossendorf, Dresden, Germany
M. Downer, Z. Ouyang, The University of Texas at Austin, Austin, TX, USA

Abstract

Optical transition radiation (OTR) beam profile monitors are widely used to measure the transverse profiles of low-charge electron bunches at advanced linear accelerator facilities such as LCLS-II and FACET-II. However, in scenarios involving strong longitudinal compression or microbunching-induced current spikes, the incoherent OTR signal—proportional to the transverse beam density—is often dominated by coherent OTR (COTR). The resulting COTR patterns exhibit complex dependencies on the full spatiotemporal structure of the beam, rendering conventional profile interpretation ineffective. In this work, we present a novel, backwards-differentiable simulation framework for COTR emission, enabling gradient-based inference of beam characteristics directly from COTR images. We further integrate this framework with the generative phase space reconstruction (GPSR) method to recover high-fidelity 4D transverse phase space distributions of strongly compressed beams. Simulation results demonstrate the ability of this approach to accurately reconstruct detailed beam structure from COTR-based diagnostics, offering a new path toward high-resolution characterization of ultrashort electron bunches.

INTRODUCTION

Optical transition radiation (OTR) beam diagnostics are a common method to diagnose the transverse profile of the beam distribution in both conventional accelerators such as LCLS or FACET-II and novel accelerators such as laser wakefield accelerators (LWFA). Generally, particle beams that intercept metallic foils emit OTR radiation, which can then be imaged using cameras. In cases where the longitudinal bunch length is longer than the imaging wavelength, the radiation is incoherent (IOTR) and thus the intensity of the transverse radiation pattern is proportional to the transverse beam profile. However, in cases where the beam is shorter than the imaging wavelength, either due to longitudinal compression in magnetic chicanes, longitudinal micro-bunching, or short pulse durations generated by LWFA sources, the emitted radiation is coherent (COTR), leading to a more complex relationship between the transverse particle distribution and transverse radiation pattern. As a result, OTR screens located in areas where short pulse durations are present tend to be corrupted by COTR, making it challenging to diagnose the transverse beam distribution.

* rroussel@slac.stanford.edu

To address this problem, we have implemented so-called backwards differentiable simulations of incoherent and coherent OTR that can be used to effectively infer transverse beam properties from beam profile measurements that contain COTR. Backwards differentiable simulations are a simulation methodology that tracks the derivatives of each individual computation to enable inexpensive computations of output gradients with respect to large numbers of input parameters. These gradients can then be used to infer beamline [1] or beam distribution properties [2] through the use of gradient-based optimization algorithms, which scale effectively to large numbers of free parameters.

In this work, we describe the implementation of differentiable COTR calculations. We then demonstrate on a synthetic test case how differentiable beam dynamics simulations containing COTR phenomena can be used to reconstruct transverse 4-dimensional phase space distribution structure of short beam distributions. This opens the door to resolving beam distribution structure in locations where diagnostics were previously unavailable, namely after longitudinal bunch compression at free electron lasers or at LWFA facilities.

DIFFERENTIABLE COTR SIMULATIONS

The goal of our simulation is to calculate the intensity distribution of both incoherent and coherent OTR signals at M wavelengths on a 2D, transverse mesh grid of $H \times W$ pixels on our diagnostic screen given a distribution of N macro-particle coordinates $X = \{\mathbf{x}_1, \mathbf{x}_2, \dots\}$ in 6D phase space. To enable backwards-differentiability we implement each stage of the OTR calculation in the Python library PyTorch [3]. We also implement the simulation in a manner such that it is vectorized, meaning that it can execute multiple, batched calculations of OTR signals for multiple incoming beam distributions at once. This leverages parallel computing capabilities of CPUs and more importantly GPUs, which PyTorch natively supports. For notation simplicity, we neglect the batch dimensions here.

We compute the incoherent and coherent portions of the OTR separately. First, we estimate the density of the beam distribution in position space $\rho(x, y, z)$ from macro-particle coordinates using the kernel density estimation technique, which is vectorized and maintains differentiability with respect to the particle coordinates. We then obtain the IOTR by integrating the beam density over the longitudinal axis, resulting in a 2D profile, $g(x, y)$. Finally, we convolve it over x and y with the OTR point spread function (PSF) [4], which

ISBN: 978-3-95450-261-5 ISSN: 2673-7000 doi: 10.18429/JACoW-NAPAC2025-MOP029

describes the OTR fluence from a single electron transiting the screen. This gives us

$$\frac{dW_{\mathrm{IOTR}}(x,y;\lambda)}{dx\,dy\,d\lambda} = g(x,y) * \mathrm{PSF}(x,y;\lambda). \tag{1}$$

The computation of the COTR follows a similar procedure, albeit with slight additional complexity due to ensemble effects from coherence. Instead of summing along the longitudinal axis, we compute a Fourier transform along this axis evaluated at $k = 2\pi/\lambda$, where λ is the measured wavelength:

$$g_{\mathrm{eff}}(x,y,\lambda) = \int \exp\left(-i\,\frac{2\pi}{\lambda}z\right)\rho(x,y,z)dz. \tag{2}$$

This complex, effective 2D profile is then convolved over x and y with the transverse electric fields responsible for the PSF, i.e. E_x^{PSF} and E_y^{PSF}, where the subscripts x and y correspond to x- and y-polarized fields and $\mathrm{PSF} = |E_x^{\mathrm{PSF}}|^2 + |E_y^{\mathrm{PSF}}|^2$. These field convolutions are computed for both polarizations and absolute value squared of these fields are summed to calculate the coherent fluence:

$$\frac{dW_{\mathrm{COTR}}(x,y;\lambda)}{dx\,dy\,d\lambda} = |g_{\mathrm{eff}}(x,y;\lambda) * E_x^{\mathrm{PSF}}(x,y;\lambda))|^2 \quad + \quad |g_{\mathrm{eff}}(x,y;\lambda)) * E_y^{\mathrm{PSF}}(x,y;\lambda))|^2. \tag{3}$$

Finally, the total fluence $W_{\mathrm{total}} = nW_{\mathrm{IOTR}} + n(n-1)W_{\mathrm{COTR}}$, where n is the number of electrons in the bunch.

Because every step — summation, tensor slicing, reshaping, and grouped convolution — is a native PyTorch operation, the entire pipeline is fully differentiable and vectorized. This design eliminates Python-level loops over wavelengths or batch elements, maximally leverages optimized fused kernels, and seamlessly supports arbitrary batching for end-to-end gradient-based optimization or uncertainty quantification.

Figure 1 shows 2-D projections of the synthetic beam which, using the convolution kernels shown in Fig. 2, are used to calculate the OTR patterns at three different wavelengths as shown in Fig. 3.

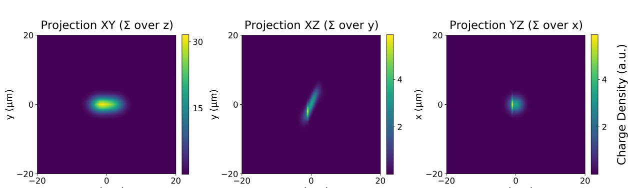

Figure 1: 2-D projections of the beam.

UTILIZING COTR SIMULATIONS TO RESOLVE 4-DIMENSIONAL PHASE SPACE DISTRIBUTION

Integrating differentiable COTR computations into the Cheetah package allows this physics phenomena to be integrated into high-performance optimization workflows, such

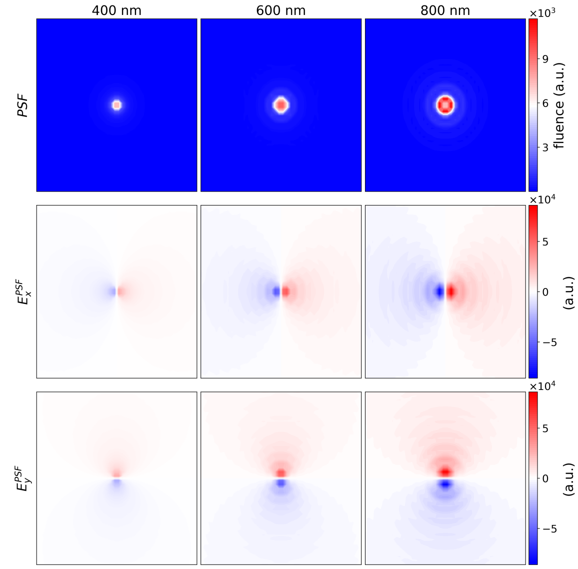

Figure 2: Point spread functions at wavelengths 400 nm, 600 nm, and 800 nm (top row). Transverse electric fields polarized in x (y) displayed in the middle (bottom) row.

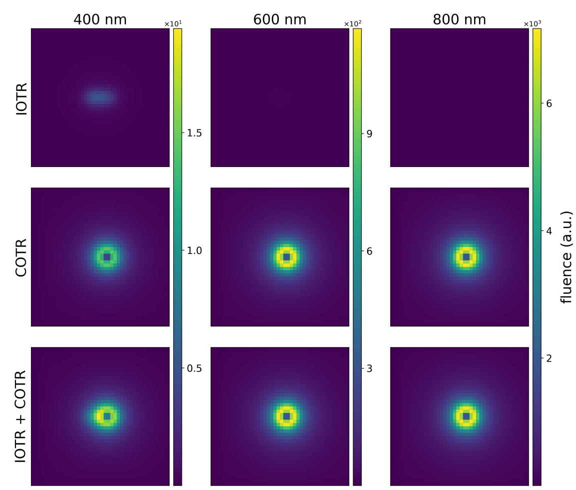

Figure 3: Forward calculated OTR from the beam distribution shown in Fig. 1. The columns depict the radiation at three different wavelengths (400 nm, 600 nm, and 800 nm). The first row shows the incoherent OTR, the second the coherent, and the third the sum of the first two rows.

as Generative Phase Space Reconstruction (GPSR) [5]. In this analysis workflow, the detailed structure of the beam distribution in position-momentum space is generated by a machine learning transformer network that is determined by fitting the parameters of the transformer such that the beam dynamics simulation predictions match experimental measurements. The transformer-based description of the beam distribution results in a large number ($\sim 10^3$) of parameters that dictate the structure of the beam distribution. Fitting these parameters to experimental measurements necessitates the use of gradient-based optimization algorithms, which is enabled by inexpensive gradient computations provided by differentiable simulations.

ISBN: 978-3-95450-261-5 ISSN: 2673-7000 doi: 10.18429/JACoW-NAPAC2025-MOP029

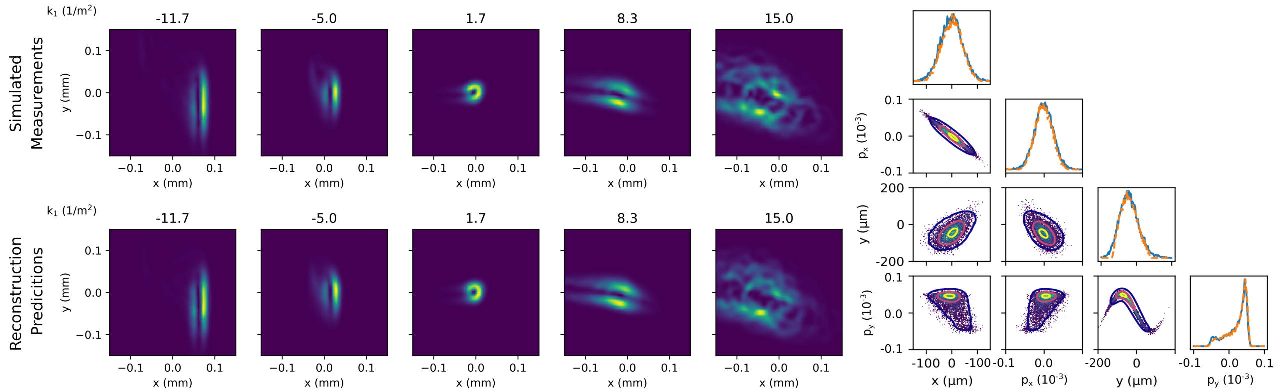

Figure 4: Comparison between GPSR reconstruction results in a synthetic test case where COTR dominates the diagnostic images. Left: Comparison between simulated measurements (top row) and reconstruction predictions (bottom row) for test quadrupole strengths. Right: Comparison of 2-D projections in transverse phase space between ground truth distribution (colormap, blue) and reconstruction (contour lines, orange).

To demonstrate the use of differentiable COTR simulations in GPSR, we created a synthetic test distribution that is tracked through a quadrupole and then a drift, finally arriving on a screen that emits COTR. For simplicity, we assume that the beam distribution is temporally coherent at visible wavelengths and the beam size is large compared to $\lambda\gamma$. Thus, the intensity of the COTR signal is $I_{COTR}(x, y) \propto |\nabla\rho(x, y)|^2$ [6]. We integrate this basic model of COTR into the differentiable beam dynamics simulation code Cheetah [1], which allows it to be integrated into the GPSR workflow.

We create a synthetic experimental dataset by scanning the quadrupole focusing strength and collecting the simulated COTR signal at the diagnostic screen. This image dataset is then used with the same differentiable simulation to reconstruct the transverse phase space distribution using GPSR. As shown in Fig. 4, the reconstruction algorithm is able to accurately reproduce the synthetic experimental images, while also correctly predicting the synthetic distribution structure.

CONCLUSION

In this work, we summarized current efforts to implement differentiable calculations of COTR in PyTorch and demonstrated that differentiable COTR computations can be used in conjunction with GPSR to accurately resolve transverse distribution structure of beams. This analysis enables a detailed understanding of the transverse phase space distribution of longitudinally compressed beams where OTR diagnostics were previously unusable. Additionally, while the example shown here demonstrates a reconstruction of the beam distribution via a multi-shot measurement, its possible to use a similar workflow to reconstruct the 3-dimensional positional distribution of the beam by observing the COTR signal at multiple wavelengths in the same way as done in [7]. Future work will aim to integrate the detailed model of IOTR / COTR presented here into the Cheetah package for performing reconstructions from experimental measurements.

ACKNOWLEDGMENTS

This work is supported by the U.S. Department of Energy, Office of Science under Contract No. DE-AC02-76SF005152.

REFERENCES

[1] J. Kaiser, C. Xu, A. Eichler, and A. Santamaria Garcia, "Bridging the gap between machine learning and particle accelerator physics with high-speed, differentiable simulations", *Phys. Rev. Accel. Beams*, vol. 27, no. 5, p. 054 601, 2024. `doi:10.1103/PhysRevAccelBeams.27.054601`

[2] R. Roussel *et al.*, "Efficient six-dimensional phase space reconstructions from experimental measurements using generative machine learning", *Phys. Rev. Accel. Beams*, vol. 27, no. 9, p. 094 601, 2024. `doi:10.1103/PhysRevAccelBeams.27.094601`

[3] A. Paszke *et al.*, "PyTorch: An imperative style, high-performance deep learning library", *Adv. Neural Inf. Process Syst.*, vol. 32, 2019. `doi:10.48550/arXiv.1912.01703`

[4] P. Karataev, A. Aryshev, S. Boogert, D. Howell, N. Terunuma, and J. Urakawa, "First observation of the point spread function of optical transition radiation", *Phys. Rev. Lett.*, vol. 107, no. 17, p. 174 801, 2011. `doi:10.1103/PhysRevLett.107.174801`

[5] R. Roussel *et al.*, "Phase Space Reconstruction from Accelerator Beam Measurements Using Neural Networks and Differentiable Simulations", *Phys. Rev. Lett.*, vol. 130, no. 14, p. 145 001, 2023. `doi:10.1103/PhysRevLett.130.145001`

[6] H. Loos *et al.*, "Observation of Coherent Optical Transition Radiation in the LCLS Linac", in *Proc. FEL'08*, Gyeongju, Korea, Aug. 2008, pp. 485–489. `https://jacow.org/FEL2008/papers/THBAU01.pdf`

[7] M. LaBerge *et al.*, "Revealing the three-dimensional structure of microbunched plasma-wakefield-accelerated electron beams", *Nat. Photonics*, pp. 1–8, 2024. `doi:10.1038/s41566-024-01475-2`